A&A 424, 993–1002 (2004)
DOI: 10.1051/0004-6361:20035902

Astronomy & Astrophysics

Spectroscopic and photometric observations of the short-period RS CVn-type star BH Virginis⋆,⋆⋆,⋆⋆⋆

D. P. Kjurkchieva[1], D. V. Marchev[1], P. A. Heckert[2], and C. A. Shower[2]

[1] Department of Physics, Shoumen University, 9700 Shoumen, Bulgaria
e-mail: [d.kyurkchieva;d.marchev]@shu-bg.net
[2] Department of Chemistry and Physics, Western Carolina University, Cullowhee, NC, 28723, USA
e-mail: heckert@wcu.edu

Received 18 December 2003 / Accepted 11 May 2004

Abstract. High-resolution spectroscopic observations around the H_α line and *BVRI* photometry from 1993 to 2003 of the eclipsing short-period RS CVn star BH Vir are presented. The simultaneous solution of our radial velocity curves and light curves yielded the following values for global parameters of the components: $M_1 = 1.173 \pm 0.006\ M_\odot$; $M_2 = 1.046 \pm 0.005\ M_\odot$; $R_1 = 1.22 \pm 0.05\ R_\odot$; $R_2 = 1.11 \pm 0.04\ R_\odot$; $i = 87.5° \pm 0.8°$. The measured rotational broadening of the spectral lines corresponds to equatorial velocities $V_1 = 79.8$ km s^{-1} and $V_2 = 68.4$ km s^{-1}. Our data reveal considerable H_α emission excess of the two stellar components. We modelled the photometric data to find the size and location of the starspots for each year. The established decreasing trend of the spot latitudes may indicate a latitudinal cycle of at least a decade.

Key words. stars: activity – stars: binaries: eclipsing – stars: binaries: spectroscopic – stars: individual: BH Vir – stars: starspots – stars: chromospheres

1. Introduction

BH Vir is a double-line eclipsing binary classified as a short-period RS CVn system (Strassmeier et al. 1993). It is a close detached binary containing main-sequence stars with rapid rotation. The observations in different spectral ranges (from X-ray to radio) indicate chromospheric-coronal radiation from these stars (Budding et al. 1982).

The light curves of BH Vir show large intrinsic variations at all phases. Photometric observations of Kitamura et al. (1957) show constant brightness between the eclipses while those of Koch (1967) reveal night-to-night changes and an extraordinarily large reflection effect (maximum distortion around phase 0.5) without a proximity effect. The light curves of Hoffmann (1982) show asymmetric primary minima, indications of ellipticity and variability of the depths of the two minima during only a few days. Xiang & Liu (1997) found a slight brightness decrease at phase 0.65. The IR light curves of BH Vir (Arevalo et al. 2002) have a shape similar to that of the UBVRI light curves (Zeilik et al. 1990). In spite of the variable light curve the orbital period of BH Vir shows no obvious changes (Xiang et al. 2000).

While dark spots can account for some of the variability, the observed brightening in some phases needs other causes (Arevalo & Lazaro 1990). Botsula (1978) attributed the remarkable intrinsic light variations of BH Vir to circumstellar material.

In contrast to almost all RS CVn systems, Abt (1965) did not detect CaII emission from BH Vir. He determined components of almost equal mass and spectral types G0V and G2V. Koch (1967) classified them as F8IV-V and G2V from UBV color index analysis while Popper (1997) obtained spectral types F8 and G5.

The IUE observations of Budding et al. (1982) revealed emission in the MgII h and k lines. The spectral observations of Lazaro & Arevalo (1997) revealed that both components of BH Vir present excess emission in the H_α line at all orbital phases with *EW* up to 0.5 Å. The phase behavior of the H_β line is similar to that of the H_α line but the emission is weaker. All the spectra of BH Vir collected in the CaII infrared triplet show emission in the two lines (8542 and 8592 Å).

⋆ Based on spectral observations collected at the National Astronomical Observatory at Rozhen and photometric observations collected at Mt. Laguna Observatory operated by San Diego State University, research was supported in part by the NATO Linkage grant No. PST.CLG.978810, grant No. 8/2003 of the Shoumen University, a Cottrell College Science Award of the Research Corporation, and grants from NASA and the Gaposchkin Fund administered by the AAS Small Grants Program.

⋆⋆ Photometric and spectroscopic data are only available in electronic form at the CDS via anonymous ftp to
cdsarc.u-strasbg.fr (130.79.128.5) or via
http://cdsweb.u-strasbg.fr/cgi-bin/qcat?J/A+A/424/993

⋆⋆⋆ Figures 2–7 and Figs. 9–16 are only available in electronic form at http://www.edpsciences.org

Lazaro & Arevalo (1997) explained the low and nearly constant line ratios $EW(H_\alpha)/EW(H_\beta)$ and $EW(8542)/EW(8492)$ as indications of optically thick formation typical of plage-like structures.

Despite the intensive photometric studies of BH Vir (Kitamura et al. 1957; Koch 1967; Botsula 1978; Hoffmann 1982; Arevalo et al. 1987; Derman et al. 1989; Arevalo & Lazaro 1990; Heckert & Summers 1994, 1995; Xiang & Liu 1997; Clement et al. 1997a) the global parameters of BH Vir are poorly determined mainly because there are only two sets of spectral observations (Abt 1965; Popper 1997). The resulting values of the mass ratio are quite different: 1.02 (Abt 1965) and 0.90 (Popper 1997), leading to different values of the star parameters. Moreover the large and fast amplitude variations prevent precise determinations of the parameters from the photometric analysis.

Accurate values of masses, radii and temperatures are needed to improve the mass-luminosity relation at the end of the Main Sequence. New radial velocity curves would provide a re-determination of the mass ratio and hence the global parameters of BH Vir. In addition, understanding the spot evolution and possibly cyclic spot behavior requires systematic regular photometry over a long time period. To these ends, we began a program of regular photometry of BH Vir from 1993 to 2003 along with spectroscopy in 2003.

2. Observations

2.1. Spectral observations

On two nights in April and five nights in May 2003 BH Vir was observed in the spectral range around the H_α line (6470–6670 Å) with resolution 0.19 Å/pixel. We used a CCD Photometrics AT200 camera with the SITe SI003AB 1024×1024 pixels chip mounted on the Coude spectrograph (grating $B\&L632/14.7°$) on the 2-m telescope of the National Astronomical Observatory at Rozhen. The seeing during the observations did not exceed 2 arcsec (FWHM). The exposure time was 20 min. The bias frames and flat-field integrations were obtained at the beginning and at the end of each night. All stellar integrations were alternated with Th-Ar comparison source exposures for wavelength calibration. The S/N ratio was around 60 in the April run and around 80–100 in the May run. β Vir, the radial velocity and nonactive standard star, was observed 2 times every night.

The spectral data were phased according to the ephemeris (Kreiner et al. 2001)

$$\mathrm{HJD(MinI)} = 2\,443\,230.6077 + 0.816871312 \times E. \quad (1)$$

We reduced the spectra in a standard way, using the PCIPS (Smirnov et al. 1992) and Rewia (Borkowski 1988) software packages, by bias subtraction, flat-field division and wavelength calibration.

The spectra at the two eclipses and quadratures are shown in Fig. 1 while Figs. 2–7 present the spectra from the different nights.

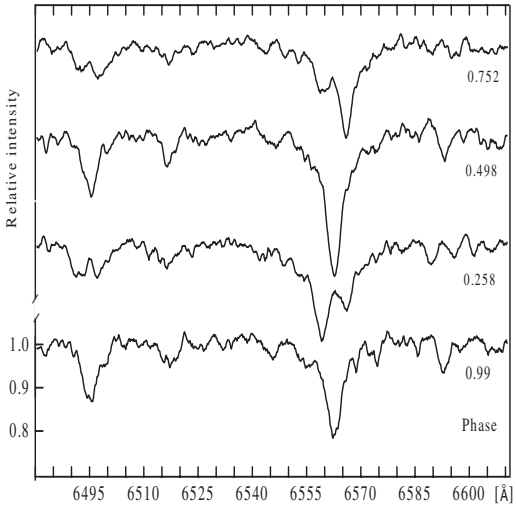

Fig. 1. The spectra of BH Vir at the eclipses and quadratures.

2.2. Photometric observations

We collected the photometric data on BH Vir with the Mt Laguna Observatory 61 cm telescope, operated by San Diego State University. The telescope has a photometer with a Hamamatsu R943-02 tube that is cooled to −15°C and operates at −1450V. The comparison star is GSC 4968 0476. Using standards of Landolt (1983) we find that the calibrated magnitudes of our comparison star are: $B = 11.01$, $V = 10.39$, $R = 10.03$, and $I = 9.69$. We collected annual sets of light curves in the *BVRI* bands from 1993 to 2003. Table 1 provides a complete observing log. The 1993 and 1994 light curves have been previously published (Heckert & Summers 1994, 1995), so they are not shown here. The 1995 through 2003 light curves are plotted in Figs. 8–16. These data are *BVRI* magnitudes in the standard Johnson-Cousins system. Because we started the photometric program before the Kreiner et al. (2001) ephemeris was available the phases are computed using (Koch 1967):

$$\mathrm{HJD(MinI)} = 2\,438\,107.19047 + 0.81687099 \times E. \quad (2)$$

(According to this ephemeris the phases of the spectral observations in Figs. 1–7 should be increased by 0.0075.)

The 1995, 1998, 2000, 2002, and 2003 light curves are the most complete and have no significant gaps. The 2001 light curves have small gaps outside the eclipses. The 1994 and 1999 light curves have small gaps during a portion of one of the eclipses but are otherwise complete. The 1993 and 1996 light curves have gaps both during one of the eclipses and out of the eclipses. The 1997 light curves are the poorest quality with significant gaps during both eclipses and out of the eclipses. The 1997 data were taken in August, near the end of the observing season for BH Vir, so we often had to observe it at higher than optimal air mass. Hence, these light curves are more noisy and less complete than the others. They do however allow us to model the changes in the spots on this system.

Table 1. Photometric observing Log.

Year	Nights of observation
1993	July 22, 24, 25, 26, 27, 28, 29, 30
1994	May 13, 14, 15, 16, 17, 20, 21
1995	April 22, 23, 24, 25, 26
1996	May 8, 11, 14, 16, 20, 21, 22, 23
1997	August 2, 4, 5, 6, 9, 11, 12, 13, 14, 16, 17
1998	May 11, 15, 17, 18, 19, 20, 21, 22, 23, 24, 25
1999	May 14, 15, 16, 17, 20, 22, 23
2000	May 21, 22, 23, 27, 28, 29, 30, 31, June 1
2001	May 17, 18, 21, 22, 23, 24, 25, 26
2002	June 9, 10, 11, 12, 13, 14, 15, 16, 17
2003	April 9, 20, 24, 25, 26, 28

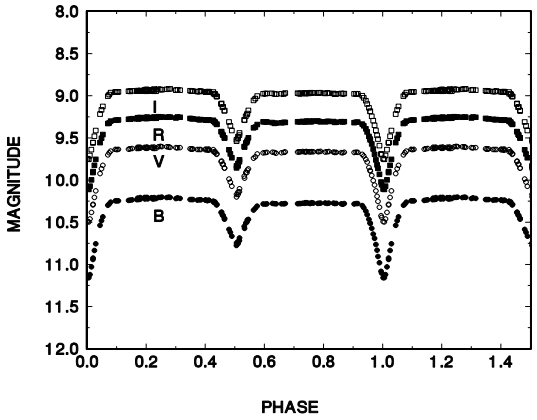

Fig. 8. The light curve of BH Vir in 1995.

3. Analysis of the observational data

3.1. Orbital variability of the spectral lines

The H_α lines of the two components of BH Vir are in absorption at all orbital phases (Fig. 1). The H_α profile of the primary star has a regular shape at most phases while that of the secondary star is distorted at most phases and has an emission core in the phase ranges 0.76–0.81, 0.11–0.18 and 0.24–0.3.

The 6495 Å line is the second strongest line of BH Vir in the observed spectral range 6470–6670 Å (Fig. 1). In contrast to the H_α line the depths of the 6495 Å line at the two eclipses are equal and the relative difference of the depths of the profiles of the two stellar components is smaller (they are even equal in strength at some phases). We also found orbital variability of this line in the short-period RS CVn-stars: CG Cyg (Kjurkchieva et al. 2003a), ER Vul (Kjurkchieva et al. 2003b), and WY Cnc (Kjurkchieva et al. 2004). Profiles of the latter had wide wings and filled-in cores. In the spectra of BH Vir this line is quite distorted by several deep and stationary features (6493, 6497.5 and 6491 Å), probably caused by interstellar or telluric absorption or both. Hence this line is not appropriate for the radial velocity measurements.

The FeI 6593 Å line is the third deepest in the spectra of BH Vir. The profiles of the two stellar components do not have wide wings and are appropriate for radial velocity measurements. The relative difference between the depths of the two lines is smaller than that of the H_α lines and they are even equal in depth at some phases.

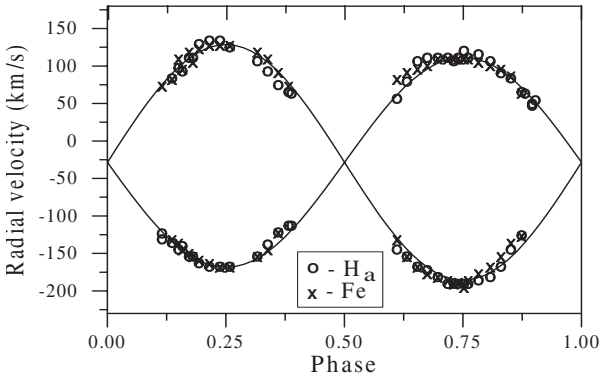

Fig. 17. Radial velocity curves of BH Vir.

3.2. Radial velocity solution

The measurement of the radial velocity of the spectral lines of the short-period RS CVn-stars is difficult due to their rotational broadening and variable blending with the surrounding metal lines (Frasca et al. 2000). Moreover the profiles are distorted by emission or absorption features. Nevertheless Hill et al. (1989) argued that for detached systems with rotational velocity <100 km s^{-1} (like BH Vir) the Gaussian approximation is very good.

We measured the radial velocities of the H_α and FeI 6593 Å lines of BH Vir by fitting their profiles with sums of two gaussians at each phase. Towards this goal we used the May spectra because of their higher quality (it should be noted there was very clear and dry weather during the entire May run of our observations).

The errors of the radial velocity do not exceed 11 km s^{-1} for the lines of the primary star and 24 km s^{-1} for the lines of the secondary star. The measured radial velocity data are given in Table 2. They were fitted by sinusoids (Fig. 17) and the solution of the radial velocity curves is: $K_1 = 140.06 \pm 0.63$ km s^{-1}; $K_2 = 157.13 \pm 0.86$ km s^{-1} ($q = 0.891$). We determined the systematic velocity of BH Vir using the observed standard star β Vir as $\gamma = -28.4$ km s^{-1}.

Our K values are almost the same as those obtained by Popper (1997) $K1 = 140.7 \pm 0.3$ km s^{-1} and $K2 = 155.9 \pm 0.5$ km s^{-1} ($q = 0.9$; $\gamma = -20.1 \pm 0.4$ km s^{-1}) while the earlier values of Abt (1965) are $K1 = 137.8$ km s^{-1}, $K2 = 135.2$ km s^{-1} ($q = 1.02$; $\gamma = -28.7$ km s^{-1}). But our γ velocity is closer to that of Abt.

3.3. Light curve solutions

To study the spot behavior in this system, we analyzed the starspots using the Information Limit Optimization Technique (ILOT) developed by Budding & Zeilik (1987). Zeilik et al. (1990) applied this technique to model the data available at that time, and discussed this technique relative to BH Vir. We use the results of this work for the initial guesses for the system

Table 2. Radial velocity data in km s^{-1}.

Phase	$V_1(H_\alpha)$	$V_2(H_\alpha)$	V_1(Fe)	V_2(Fe)
0.115	–115.18		–107.27	88.37
0.136	–119.76	99.64	–116.37	97.47
0.150	–128.90	113.36	–120.92	124.77
0.158	–124.33	108.78	–130.02	111.12
0.172	–138.04	127.07	–134.57	133.87
0.180	–138.04	127.07	–139.12	120.22
0.193	–147.18	145.35	–143.67	138.42
0.215	–151.75	149.92	–148.22	142.97
0.237	–151.75	149.92	–152.77	142.97
0.258	–151.75	140.78	–152.77	142.97
0.316	–138.04	122.50	–139.12	133.87
0.338	–122.04	108.78	–130.02	124.77
0.360	–106.04	90.50	–107.27	106.57
0.382	–96.90	81.36		88.37
0.388	–96.90			79.27
0.611	72.22	–128.90	97.47	–116.37
0.632	95.07	–138.04	106.57	–139.12
0.654	122.50	–151.75	111.12	–152.77
0.675	127.07	–156.32	115.67	–161.87
0.697	127.07	–165.47	124.77	–166.42
0.718	127.07	–174.61	124.77	–170.97
0.731	122.50	–174.61	124.77	–175.52
0.740	127.07	–174.61	124.77	–173.25
0.752	136.21	–174.61	124.77	–180.07
0.761	127.07	–174.61	124.77	–170.97
0.783	131.64	–170.04	120.22	–161.87
0.808	122.50	–165.47	115.67	–152.77
0.830	106.50	–151.75	111.12	–139.12
0.851	99.64	–128.76	102.02	–120.92
0.874	81.36	–110.00	79.27	–111.82

parameters in our models. The basic procedure for the ILOT is to fit the data to eclipsing binary parameters including orbital properties and properties of the individual stars in the system. Then the eclipse effects are removed from the data under the assumption that eclipse and spot effects in the light curves are separable. After modelling the spot parameters with the eclipse effects removed, the spot effects are removed to perform clean fits for the system parameters.

Rather than simply computing a χ^2, the ILOT computes a curvature Hessian to check the determinacy of the solution. If the solution is determinant, the program computes formal error estimates. If not, the program indicates that the solution is not determinant. Hence the ILOT does not allow one to attempt to extract more information from the data than they contain. The latitude is the most difficult spot parameter to fit. In the cases where we were unable to find a determinant solution for all the spot parameters including the latitude we fixed the latitude at the value to which it seemed to be trying to converge in trial fits and did not report an error estimate for the latitude. Also note that with a 90° inclination (or very nearly so) there

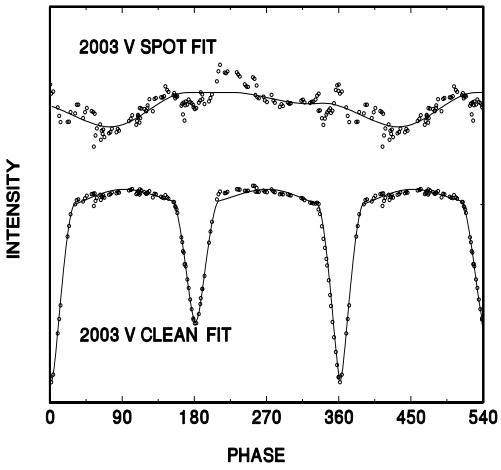

Fig. 18. Spot and clean fits for the 2003 photometry.

is a north-south ambiguity for the latitudes. We report all latitudes as northern hemisphere, but the spot could be in either hemisphere.

The modelling results are given in Tables 3 and 4. In addition Fig. 18 shows the fits for the year 2003. For the spot fits in Table 3, λ, β, and γ are the longitude, latitude, and radius of the spots in degrees. The longitude is defined so that 0° corresponds to the predicted center of the primary eclipse and increases with phase. The latitude is measured north or south of the equator, however we report only positive latitudes. The ILOT fits the spot parameters at each wavelength independently. Hence comparing the spot fits at different wavelengths provides a feel for the validity of the fit. Comparing the modelled radius of 0K spot fits in the R or I bands to that in the B or V bands allows an estimate of the spot temperature. The reported spot temperatures are the average of the four possible estimates. These spot temperatures compare to our adopted star temperatures of 6000 K and 5850 K. The 1994 spot fits are from Heckert & Summers (1995). The 1993 fits differ slightly from those of Heckert & Summers (1994) because we redid the fits with updated star temperatures.

For the clean fits in Table 4, L_1 and L_2 are the fractional luminosities of the primary and secondary stars. They are normalized to sum to approximately but not exactly 1 because the spots affect the normalization by a small amount. Representing the primary star radius, r_1 is in units of the semi-major axis. The ratio of the radii is $k = r_2/r_1$, and the mass ratio is $q = m_2/m_1$. The inclination, i, is in degrees. For the clean fits we adopted a mass ratio of $q = 0.891$, as determined by our spectroscopy.

3.4. Global parameters

Using our values of K_1 and K_2 and the photometrically determined value of the orbital inclination $i = 87.5°$ (Table 4), we obtained the masses of the star components of BH Vir: $M_1 = 1.173 \pm 0.006\ M_\odot$ and $M_2 = 1.046 \pm 0.005\ M_\odot$.

On the basis of our radial velocity solution and the averaged values of the relative star radii (Table 4) $r_1 = 0.255$ and $r_2 = 0.230$ from the light curve solutions we calculated the absolute

Table 3. Spot parameters.

Filter	λ_1	β_1	γ_1	λ_2	β_2	γ_2	$T_{\rm Spot}$(K)	χ^2
1993	N = 60							
B	282.4 ± 4.8	79.1 ± 8.5	37.2 ± 13.9				3830 ± 200	65.2
V	280.3 ± 5.0	78.2 ± 6.8	34.5 ± 9.9				3830 ± 200	44.8
R	288.4 ± 5.9	79.1 ± 1.4	33.0 ± 0.8				3830 ± 200	30.6
I	281.1 ± 6.1	79.8 ± 6.7	33.6 ± 11.7				3830 ± 200	43.1
1994	N = 147							
B	45.2 ± 5.3	45(fixed)	13.8 ± 0.5	133.1 ± 4.3	45(fixed)	15.8 ± 0.5	4050 ± 540	156.3
V	53.3 ± 6.8	45(fixed)	12.3 ± 0.7	142.5 ± 6.4	45(fixed)	13.4 ± 0.8	4050 ± 540	98.4
R	50.5 ± 15.2	45(fixed)	10.5 ± 1.6	138.5 ± 11.6	45(fixed)	13.1 ± 1.5	4050 ± 540	21.2
I	42.6 ± 15.3	45(fixed)	10.8 ± 1.5	145.0 ± 10.4	45(fixed)	14.0 ± 1.4	4050 ± 540	16.9
1995	N = 141							
B	267.0 ± 2.2	74.1 ± 2.4	36.5 ± 2.8				4070 ± 340	66.3
V	269.3 ± 2.6	73.3 ± 2.7	32.2 ± 2.7				4070 ± 340	71.9
R	266.9 ± 3.1	70.0 ± 3.0	27.5 ± 3.2				4070 ± 340	48.0
I	270.0 ± 3.6	71.1 ± 3.6	26.0 ± 2.8				4070 ± 340	55.3
1996	N = 138							
B	68.3 ± 10.6	45(fixed)	8.2 ± 0.9				4800 ± 370	383.2
V	77.1 ± 28.6	45(fixed)	6.4 ± 1.2				4800 ± 370	336.3
R	49.4 ± 11.8	44.5 ± 63.0	5.9 ± 4.3				4800 ± 370	323.6
I	54.1 ± 16.8	52.4 ± 66.3	6.3 ± 5.9				4800 ± 370	292.9
1997	N = 65							
B	283.8 ± 4.6	4.5 ± 2.2	11.0 ± 1.2				5330 ± 270	229.3
V	252.0 ± 8.5	74.3 ± 6.5	25.7 ± 6.1				5330 ± 270	227.5
R	269.9 ± 11.6	35.9 ± 110.3	8.5 ± 8.1				5330 ± 270	89.0
I	216.1 ± 15.9	52.4 ± 56.4	9.4 ± 7.4				5330 ± 270	248.4
1998	N = 137							
B	120.3 ± 3.3	31.6 ± 15.6	14.3 ± 2.0	28.2 ± 9.5	22.9 ± 34.2	7.8 ± 1.8	3680 ± 180	304.6
V	118.7 ± 4.1	5.0 ± 39.5	11.9 ± 1.0	37.7 ± 10.6	41.9 ± 55.9	9.3 ± 6.2	3680 ± 180	224.4
R	126.7 ± 3.7	2.5 ± 33.9	11.8 ± 0.7	34.0 ± 10.8	45.5 ± 33.7	8.4 ± 3.5	3680 ± 180	192.2
I	127.0 ± 4.5	3.7 ± 74.0	11.2 ± 1.2	37.9 ± 9.5	48.0 ± 29.7	10.3 ± 3.8	3680 ± 180	190.0
1999	N = 132							
B	247.2 ± 3.8	7.5 ± 47.9	11.3 ± 0.9	136.7 ± 8.4	33.5 ± 46.9	8.1 ± 3.4	4220 ± 180	234.7
V	246.1 ± 4.6	10.1 ± 61.4	10.5 ± 14.6	141.5 ± 11.5	20.7 ± 32.0	5.9 ± 1.4	4220 ± 180	121.9
R	245.3 ± 6.4	23.2 ± 12.8	9.2 ± 1.1	139.4 ± 11.6	2.0 ± 25.1	6.6 ± 1.1	4220 ± 180	122.3
I	242.6 ± 8.2	13.6 ± 40.5	9.1 ± 1.5	140.1 ± 12.9	2.5 ± 47.9	6.1 ± 1.2	4220 ± 180	100.6
2000	N = 153							
B	128.2 ± 5.2	48.5 ± 41.2	14.9 ± 9.6	43.7 ± 14.8	56.0 ± 23.2	8.8 ± 4.1	4290 ± 240	192.3
V	132.0 ± 6.2	33.4 ± 24.9	11.5 ± 2.5	50.2 ± 12.1	53.4 ± 20.4	10.0 ± 3.6	4290 ± 240	104.5
R	130.0 ± 7.8	49.9 ± 17.2	11.6 ± 2.8	52.4 ± 12.3	56.3 ± 24.5	10.1 ± 4.2	4290 ± 240	86.3
I	136.6 ± 10.6	60.5 ± 14.3	12.9 ± 3.5	54.6 ± 12.5	55.2 ± 28.0	9.9 ± 4.4	4290 ± 240	70.7
2001	N = 144							
B	283.1 ± 2.7	0.0 ± 24.2	11.4 ± 0.4	43.1 ± 4.9	0.0±22.3	8.3 ± 0.7	3930 ± 380	265.8
V	286.2 ± 4.0	0.05 ± 31.4	10.3 ± 0.5	44.7 ± 7.4	0.0 ± 39.1	7.1 ± 0.9	3930 ± 380	146.3
R	292.3 ± 4.4	10.1 ± 65.4	10.9 ± 1.7	47.3 ± 9.3	0.0 ± 33.9	6.6 ± 1.1	3930 ± 380	131.9
I	288.1 ± 7.0	0.0 ± 84.4	9.0 ± 0.7	43.9 ± 9.7	0.0 ± 34.1	6.3 ± 1.2	3930 ± 380	110.2
2002	N = 138							
B	305.5 ± 3.7	0.0 ± 38.3	9.7 ± 0.5	71.4 ± 4.3	26.8 ± 33.6	11.1 ± 3.0	3240 ± 140	270.9
V	307.4 ± 4.3	11.2 ± 48.1	9.9 ± 1.5	69.8 ± 5.1	36.4 ± 22.8	11.5 ± 2.8	3240 ± 140	149.3
R	307.5 ± 4.8	0.1 ± 45.2	9.3 ± 0.7	69.2 ± 6.1	0.0 ± 27.5	9.3 ± 0.7	3240 ± 140	140.4
I	313.7 ± 6.7	15.5 ± 67.8	9.4 ± 2.3	72.0 ± 9.3	30.2 ± 21.1	9.5 ± 1.6	3240 ± 140	101.3
2003	N = 132							
B	72.7 ± 3.0	11.1 ± 67.4	11.9 ± 2.0	320.1 ± 7.1	0.5 ± 24.3	6.5 ± 0.8	3490 ± 150	200.3
V	74.0 ± 3.6	11.9 ± 43.2	12.0 ± 1.9	323.8 ± 7.6	2.5 ± 34.1	6.7 ± 0.9	3490 ± 150	152.6
R	74.6 ± 5.5	7.9 ± 30.5	11.2 ± 0.9	328.3 ± 10.6	1.1 ± 29.9	6.0 ± 1.1	3490 ± 150	103.0
I	73.4 ± 6.1	8.3 ± 15.5	10.8 ± 0.7	326.3 ± 12.0	1.7 ± 29.1	5.8 ± 1.3	3490 ± 150	121.0

Table 4. Clean parameters.

Filter	L_1	$k(=r_2/r_1)$	r_1	i°	L_2	χ^2
1994	N = 147					
B	0.651 ± 0.018	0.923 ± 0.035	0.243 ± 0.005	86.7 ± 0.4	0.330 ± 0.020	125.5
V	0.627 ± 0.023	0.936 ± 0.043	0.244 ± 0.005	86.8 ± 0.4	0.356 ± 0.024	86.0
R	0.621 ± 0.031	0.918 ± 0.059	0.249 ± 0.008	87.3 ± 0.7	0.362 ± 0.032	69.5
I	0.608 ± 0.037	0.924 ± 0.071	0.248 ± 0.009	87.0 ± 0.6	0.377 ± 0.038	55.1
1995	N = 141					
B	0.616 ± 0.024	0.972 ± 0.045	0.245 ± 0.006	86.0 ± 0.3	0.365 ± 0.025	60.7
V	0.584 ± 0.029	0.982 ± 0.056	0.245 ± 0.007	86.4 ± 0.3	0.395 ± 0.030	51.8
R	0.626 ± 0.012	0.879 ± 0.023	0.259 ± 0.003	87.8 ± 0.5	0.353 ± 0.014	33.2
I	0.578 ± 0.033	0.945 ± 0.064	0.252 ± 0.008	87.2 ± 0.5	0.401 ± 0.035	41.3
1996	N = 138					
B	0.647 ± 0.015	0.898 ± 0.031	0.250 ± 0.004	87.4 ± 0.5	0.307 ± 0.017	371.3
V	0.632 ± 0.017	0.886 ± 0.034	0.257 ± 0.005	87.5 ± 0.6	0.324 ± 0.019	331.6
R	0.615 ± 0.008	0.874 ± 0.014	0.258 ± 0.002	88.2 ± 0.4	0.332 ± 0.009	321.3
I	0.604 ± 0.008	0.878 ± 0.016	0.263 ± 0.003	88.4 ± 0.7	0.352 ± 0.010	291.9
1998	N = 137					
B	0.585 ± 0.018	1.008 ± 0.037	0.243 ± 0.005	86.7 ± 0.3	0.386 ± 0.019	275.3
V	0.606 ± 0.018	0.920 ± 0.035	0.253 ± 0.005	87.5 ± 0.5	0.371 ± 0.019	198.9
R	0.576 ± 0.022	0.960 ± 0.043	0.250 ± 0.006	87.4 ± 0.4	0.400 ± 0.023	142.9
I	0.554 ± 0.027	0.972 ± 0.052	0.249 ± 0.007	87.4 ± 0.3	0.418 ± 0.028	154.1
1999	N = 132					
B	0.657 ± 0.015	0.877 ± 0.029	0.262 ± 0.004	87.1 ± 0.6	0.321 ± 0.017	196.0
V	0.637 ± 0.007	0.862 ± 0.013	0.263 ± 0.002	88.1 ± 0.5	0.338 ± 0.008	96.9
R	0.619 ± 0.032	0.883 ± 0.060	0.261 ± 0.007	87.8 ± 1.3	0.366 ± 0.033	104.1
I	0.620 ± 0.006	0.864 ± 0.012	0.265 ± 0.002	88.1 ± 0.4	0.363 ± 0.008	86.5
2000	N = 153					
B	0.556 ± 0.019	1.031 ± 0.037	0.243 ± 0.005	86.1 ± 0.2	0.417 ± 0.020	219.5
V	0.605 ± 0.024	0.935 ± 0.046	0.250 ± 0.006	87.3 ± 0.5	0.376 ± 0.025	93.3
R	0.620 ± 0.029	0.885 ± 0.058	0.258 ± 0.006	88.4 ± 2.1	0.363 ± 0.030	77.2
I	0.589 ± 0.032	0.934 ± 0.062	0.252 ± 0.008	87.5 ± 0.6	0.395 ± 0.033	65.3
2001	N = 144					
B	0.686 ± 0.005	0.803 ± 0.006	0.266 ± 0.002	90.0 ± 3.3	0.297 ± 0.006	173.6
V	0.636 ± 0.021	0.876 ± 0.039	0.255 ± 0.005	87.0 ± 0.5	0.348 ± 0.022	106.9
R	0.646 ± 0.006	0.842 ± 0.009	0.259 ± 0.002	88.2 ± 0.5	0.342 ± 0.007	100.4
I	0.629 ± 0.007	0.850 ± 0.011	0.257 ± 0.002	88.6 ± 0.8	0.355 ± 0.008	95.3
2002	N = 138					
B	0.695 ± 0.009	0.835 ± 0.018	0.263 ± 0.002	88.2 ± 1.0	0.280 ± 0.011	209.0
V	0.656 ± 0.022	0.866 ± 0.042	0.262 ± 0.005	87.6 ± 0.9	0.327 ± 0.022	100.9
R	0.612 ± 0.021	0.927 ± 0.040	0.257 ± 0.005	87.0 ± 0.4	0.371 ± 0.022	98.9
I	0.637 ± 0.009	0.860 ± 0.014	0.264 ± 0.002	88.4 ± 0.7	0.350 ± 0.010	78.2
2003	N = 132					
B	0.673 ± 0.014	0.872 ± 0.026	0.257 ± 0.003	86.6 ± 0.4	0.300 ± 0.015	116.1
V	0.651 ± 0.014	0.865 ± 0.026	0.259 ± 0.003	86.9 ± 0.5	0.323 ± 0.015	88.7
R	0.630 ± 0.021	0.881 ± 0.040	0.260 ± 0.005	86.9 ± 0.6	0.344 ± 0.023	61.1
I	0.626 ± 0.020	0.869 ± 0.037	0.261 ± 0.005	87.2 ± 0.6	0.350 ± 0.021	87.0
Mean		0.903 ± 0.051	0.255 ± 0.007	87.5 ± 0.8		

Table 5. Global parameters of BH Vir.

i°	q	r_1	r_2	$T_1(K)$	$T_2(K)$	L_1^V	$R_1(R_\odot)$	$M_1(M_\odot)$	$M_2(M_\odot)$	References
	1	0.26	0.25				1.16	0.9	0.9	Guiricin et al. (1984)
87	0.98	0.25	0.25	6000	5500	0.58	1.18	1.00	0.98	Budding & Zeilik (1987)
87.7	1.03						1.05	0.87	0.9	Strassmeier et al. (1988)
87	1.02	0.256	0.235	6000	5850	0.61	1.20	1.02	1.043	Zeilik et al. (1990)
83.4	0.97	0.26	0.24			0.67	1.17	0.85	0.83	Zhai et al. (1990)
87		0.245	0.225			0.63				Heckert & Summers (1995)
87	0.903	0.26	0.237	6095	5520	0.65	1.25	1.165	1.052	Popper (1997)
87.4	0.894	0.263	0.235	6158	5607		1.25	1.133	1.013	Clement et al. (1997)
86.5		0.255	0.235	6100	5800	0.61				Arevalo et al. (2002)
87.4	0.97	0.255	0.232	6000	5500	0.63				Xiang et al. (2000)
87.6	0.891	0.256	0.235	6000	5850	0.65	1.225	1.173	1.046	this paper

star radii: $R_1 = 1.22 \pm 0.05\ R_\odot$ and $R_2 = 1.11 \pm 0.04\ R_\odot$ ($k = R_2/R_1 = 0.91$).

The radii of the star components of BH Vir corresponding to our values of the stellar masses on the mass-radius relation for ZAMS stars are $R_1 = 1.10\,R_\odot$ and $R_2 = 1.00\,R_\odot$. This means that the two stellar components of BH Vir are oversized for their masses by around 10%.

Table 5 summarizes the global parameters of the binary system BH Vir determined by different authors.

We determined the rotational broadening of the FeI lines with the same procedure as that used for the star SV Cam (Kjurkchieva et al. 2002), i.e. by fitting the central parts of their profiles with 6th-order polynomials and measuring the half width of these fits at the continuum level. The measured values correspond to equatorial velocities $V_1 = 79.8 \pm 4.5\ \mathrm{km\,s^{-1}}$ and $V_2 = 68.4 \pm 4.5\ \mathrm{km\,s^{-1}}$ (using $i = 87.5^\circ$ from our photometric analysis). For comparison Popper (1997) determined $V_1 = 76\ \mathrm{km\,s^{-1}}$ and $V_2 = 69\ \mathrm{km\,s^{-1}}$ while Abt (1965) calculated a projected rotational velocity of $90 \pm 15\ \mathrm{km\,s^{-1}}$.

4. Activity of the star components

4.1. Spectral appearances (signs)

Different indicators of stellar activity are introduced by analogy to the Sun. The large variety of stars allows us to search for a relationship between the spatial, time and energetic scales of their level of activity and the global parameters (for instance Wilson-Bappu effect). On the other hand the study of stellar activity is the basis for the improvement of the magnetic-dynamo theory and for the establishment of criteria for solar activity forecasts.

The analysis of the orbital variability of the spectra yields information about the dominant sources of the spectral lines as well as about the locations of the active regions in binary systems. We observed BH Vir spectroscopically around the H_α line because it is a spectroscopic indicator of chromospheric activity (Zarro & Rogers 1983; Herbig 1985; Frasca & Catalano 1994; Strassmeier et al. 1990). The H_α emission excess in the active stars may appear as a H_α line above the continuum or as a weak absorption line with filled-in core. The level of star activity can be estimated from the value of the H_α emission excess.

To obtain the H_α emission excess of the stellar components of BH Vir we used the spectra of the nonactive F9V star β Vir (HD 102870). We fit its H_α line with a Voigt profile with *EW* (equivalent width) equal to that of β Vir (*EW* = 3.25 Å) and with rotational broadening equal to that of the primary star of BH Vir (Fig. 19a, below). Then the difference *EE*(0.5) between this Voigt fit and the H_α line of BH Vir at phase 0.5 is just equal to the H_α emission excess *EE1* of the primary component because: (a) the secondary star is invisible in the middle of the secondary eclipse due to the high orbital inclination of the system; (b) the spectral types of the primary star of BH Vir and β Vir are the same. The result of this procedure is shown at the top of Fig. 19a. The measured *EW* of *EE1* is 0.52 Å.

The application of this procedure to the FeI (*EW* = 0.213 Å) line is shown in Fig. 19b with three parts similar to those in Fig. 19a. We see (at the top of Fig. 19b) that the difference between the profile of BH Vir and the rotationally broadened profile of β Vir is 0 to within the errors. This result presents a test of the reliability of the procedure used for the determination of the H_α emission excess.

In order to obtain the H_α emission excess of the secondary star *EE2* of BH Vir we applied the same procedure to phase 0.0 (the middle of the primary eclipse). The total emission excess at this phase, *EE*(0), is shown at the top of Fig. 20. The difference between *EE*(0) and *EE1* gives *EE2* (Fig. 20, bottom). The measured *EW* of *EE2* is 0.84 Å. Note that we have also observed the non-active star 16 Cnc. Its spectral type G5 is closer to that of the secondary star of BH Vir. However it turns out that the *EW* of its H_α line is bigger (3.67 Å) than that of β Vir, which is the opposite of the expected relation for their spectral types. Hence to infer the emission excesses of the two components of BH Vir we used only the H_α line of β Vir.

The larger H_α emission excess of the secondary star compared to the primary star is clearly visible in the spectra of BH Vir. Figures 2–7 show smaller differences in the depths of the spectral profiles of the two star components of the lines excluding Hα. Moreover, the H_α emission excess of the secondary star of BH Vir is also visible in the presence of emission cores at most phases in Figs. 2–7.

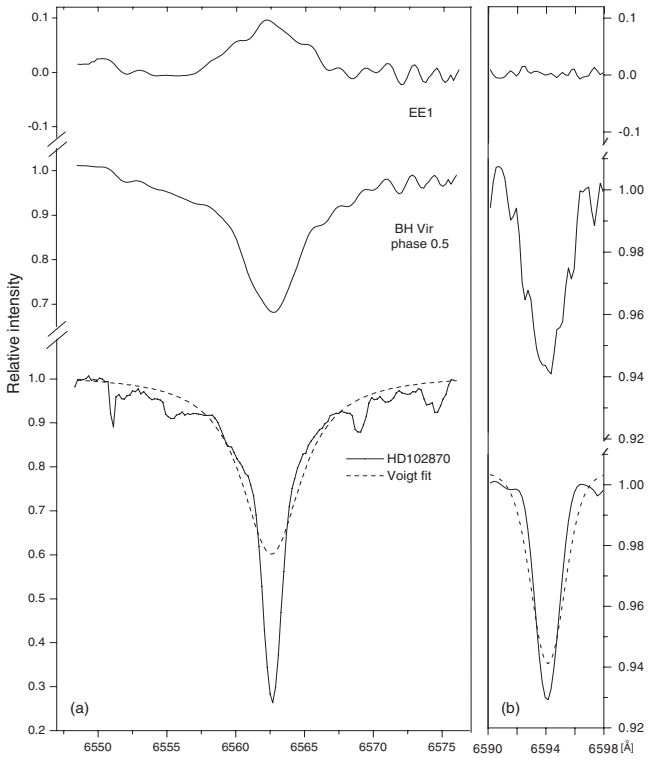

Fig. 19. a) Determination of the Hα emission excess of the primary component of BH Vir; **b)** test of the procedure with the FeI line.

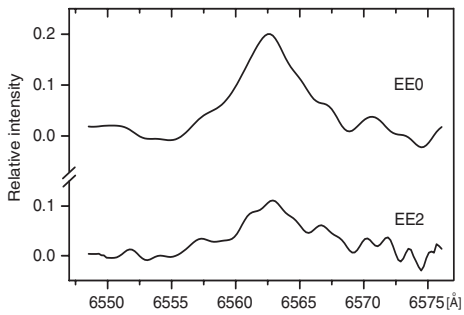

Fig. 20. The H_α emission excess of the secondary component of BH Vir.

The H_α emission excess of the stellar components of BH Vir is a sign of their chromospheric activity.

The measured H_α emission excesses at the two quadratures of BH Vir are not equal: $EE(0.75)$ = 1.2 Å, $EE(0.25)$ = 0.7 Å from May 9 but $EE(0.25)$ = 1.2 Å from April 8. The different values of the emission excesses at the two quadratures mean that the distribution of the active areas on the stellar chromospheres is not homogeneous.

The H_α absorption line from the primary star is shallow for its spectral type, as can be seen from Table 6. This table presents the temperatures of the primary stars and depths of their line centers relative to the local continuum of other short-period RS CVn stars observed with the same equipment. The values given in the table are those measured at quadratures and converted according to the relative contribution of the primary star.

Table 6. Depth of the H_α line of the primary components of of some short-period RS CVn stars.

Star	XY UMa	SV Cam	RT And	BH Vir
$T_{\rm eff}$ (K)	5780	5800	6150	6100
$d_{\rm obs}$	0.31	0.32	0.28	0.22

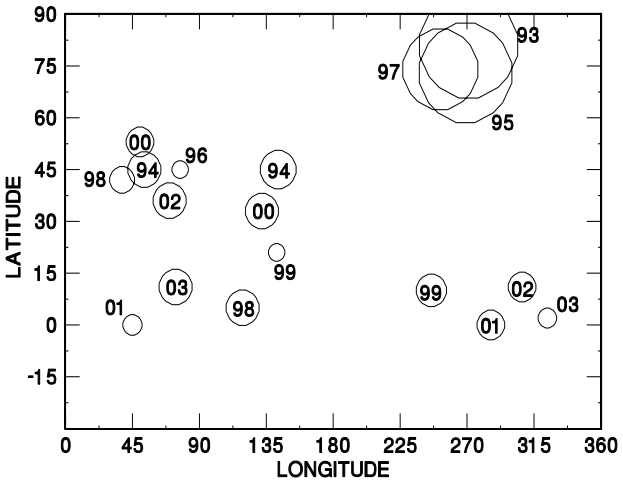

Fig. 21. Locations of the spots of BH Vir from 1993 to 2003.

Lazaro & Arevalo (1997) also found excess emission in the H_α line from both components of BH Vir at all orbital phases. They concluded that the emission excess is greater for the primary star because the *EW* of the total H_α emission is smaller at the primary eclipse than at the secondary one.

4.2. Photometric appearances

Most authors attribute the light curve distortions of BH Vir to the presence of cool (with temperature contrast 800–1400 K) photospheric regions on the primary's surface (Scaltriti et al. 1985; Budding & Zeilik 1987; Zeilik et al. 1990; Zhai et al. 1990; Heckert & Summers 1994, 1995) while Xiang et al. (2000) reproduced the 1963–64 light curves by cool spots on both components and the 1991 light curves by one active region on the secondary star.

Zeilik et al. (1990) find that the spots for BH Vir tend to occur in rather wide Active Longitude Belts (ALBs) at 90 and 270 degrees. Zeilik et al. (1989) address in detail whether this tendency, also observed in RT And, is real or an artifact of the modelling technique. BH Vir is similar enough to RT And that their arguments that this tendency is real also apply to BH Vir. This tendency also holds on other short period RS CVn systems; however, it is a tendency, not an absolute rule for these systems as demonstrated by Heckert (2001) for WY Cnc. Figure 21 shows a mercator projection of the *V* band spot locations from 1993 to 2003. BH Vir still shows this tendency towards ALBs (Fig. 22). The spots can occur at all latitudes, however we note that the highest latitude spots are in the 270° ALB. We also note that the 90° ALB does not seem to confine the spots as well as the 270° ALB. Heckert et al. (1998) note similar trends in WY Cnc.

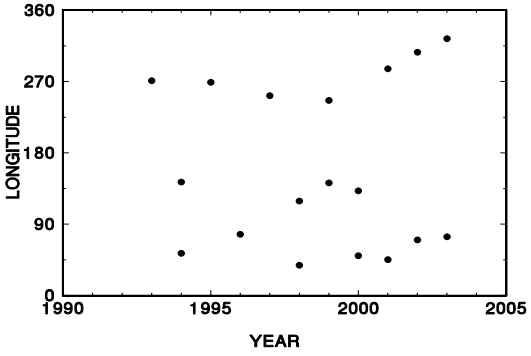

Fig. 22. Longitudes of the spots of BH Vir from 1993 to 2003.

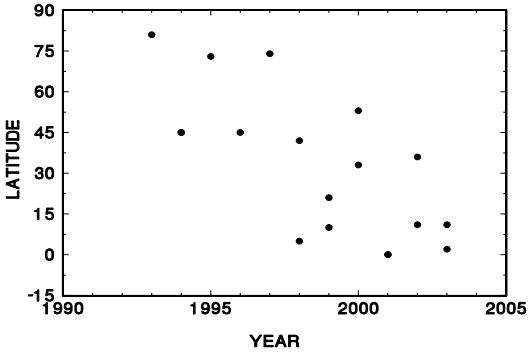

Fig. 23. Latitudes of the spots of BH Vir from 1993 to 2003.

Examination of Fig. 22 shows that during the 1990s the spotted regions had a tendency to oscillate between ALBs from year to year. With the new millennium there is a greater tendency to have one spotted region in each ALB. This longitudinal behavior suggests the possibility of some type of two-year periodicity with the additional possibility of two not quite equal superimposed periodicities.

Figure 23 plots the spot latitude as a function of time. While interpreting this figure, one must keep in mind that the latitude is the hardest spot parameter to fit. Hence the formal errors in the latitudes (Table 3) are often quite large. With this caveat, note that despite considerable scatter there seems to be a trend towards decreasing spot latitude from 1993 to 2003. If at some point we observe high latitude spots followed by a similar decreasing trend over a decade or so, we would have behavior similar to the well known butterfly diagram in the Sun. Heckert (2001b) notes the possibility of a similar latitudinal cycle in WY Cnc. Continued systematic observations over several decades are clearly needed to test the hypothesis that these stars have latitudinal spot cycles similar to the Sun's.

There appears to be a minimum in the spotted area during 1996. Analysis of these light curves reveals only one relatively small spot. In fact these data were difficult to fit. Initial attempts gave spot solutions with radii less than zero, clearly a physical impossibility, suggesting that to within the modelling errors BH Vir might have been very nearly unspotted during this epoch. Note that the 1996 data are bright during the out of eclipse phases compared to other years. Hence there really was a minimum in the spotted area rather than a longitudinal dispersal of the spots. Photometric modelling is not sensitive to spots that are evenly dispersed in longitude.

BH Vir does not seem to display secular luminosity variations similar to those observed in WY Cnc (Kjurkchieva et al. 2003c; Heckert 2001a, and references therein), which include the secondary eclipse. Even a cursory examination of the light curves of these systems reveals that WY Cnc has very shallow secondary eclipses compared to the primary eclipses. BH Vir on the other hand has relatively deeper secondary eclipses. Heckert & Ordway (2002) note secular luminosity variations on UV Psc, which has secondary eclipses that are relatively shallower than in BH Vir, but not as shallow as those in WY Cnc. Could the different relative luminosities of the two stars in these short period RS CVn systems be in some way related to the secular luminosity variations? Shallow secondary eclipses are of course indicative of various physical properties of the stars, such as spectral class, temperature, etc. Comparing similar stars, BH Vir and ER Vul both have G class secondaries. WY Cnc has an M class secondary. CG Cyg, SV Cam, RT And, UV Psc, and XY UMa all have K class secondaries. The secondary for UV Psc is luminosity class IV; the others are class V. It is possible that the lower mass or luminosity of these late secondaries in some way enhances the luminosity changes in the primary that are associated with the magnetic cycle relative to such luminosity changes associated with the Sun's magnetic cycle. Apparently this effect is smaller if the secondary is an earlier, more massive, more luminous star. The presence or absence of a third body in the system may also affect the luminosity changes with the magnetic cycle in some way.

5. Conclusion

The main results of our spectroscopic and photometric observations of BH Vir and their analysis might be summarized as follows:

Using the radial velocity curves and the photometrically determined mean values of the inclination and relative star radii, we obtained the following values of the global parameters of the system: $M_1 = 1.17\ M_\odot$; $M_2 = 1.05\ M_\odot$; $R_1 = 1.22\ R_\odot$; $R_2 = 1.11\ R_\odot$; $i = 87.5°$.

Our spectral observations revealed a large H_α emission excess of the two stellar components of BH Vir. The similar spectral behavior of the two components of BH Vir is not surprising because of their similar spectral type as opposed to the classical long-period RS CVn systems.

The out of eclipse light variations can be explained by the presence of one or two cool spotted areas. The spot latitudes may show a portion of a latitudinal cycle similar to that found in the Sun.

Acknowledgements. The authors are very grateful to the referee, Dr. C. Lazaro, whose recommendations and suggestions led to considerable improvement of this paper.

References

Abt, H. 1965, PASP, 77, 367
Arevalo, M., Robayna, B., Fuensalida, J., & Bedford, D. 1987, IBVS, No. 3177

Arevalo, M., & Lazaro, C. 1990, Ap&SS, 169, 245
Arevalo, M., Lazaro, C., Barrera, E., & Dominguez, R. 2002, IBVS, No. 5222
Borkowski, G. 1988, Internal report of Astron. Inst. in Torun, Poland
Budding, E., Kadouri, T., & Gimenez, A. 1982, A&AS, 88, 453
Budding, E., & Zeelik, M. 1987, ApJ, 319, 827
Clement, R., Reglero, V., Garcia, M., et al. 1993, in Inside the Stars, IAU Coll., 137, 386
Clement, R., Garcia, M., Reglero, V., et al. 1997a, A&AS, 123, 1
Clement, R., Garcia, M., Reglero, V., et al. 1997b, A&AS, 123, 59
Clement, R., Reglero, V., Garcia, M., Fabregat, J., & Suso, J. 1997c, A&AS, 124, 499
Derman, E., Akalin, A., & Demircan, O. 1989, IBVS, No. 3404
Frasca, A., & Catalano, S. 1994, A&A, 284, 883
Frasca, A., Marino, C., Catalano, S., & Marilli, E. 2000, A&A, 358, 1007
Giuricin, G., Mardirossian, F., & Mezzetti, M. 1984, MNRAS, 206, 305
Heckert, P. 2001a, AJ, 121, 1076
Heckert, P. 2001b, A&AS, 198, 4607
Heckert, P., & Ordway, J. 2002, A&AS, 200, 0801
Heckert, P., & Summers, D. 1994, IBVS, No. 4062
Heckert, P., & Summers, D. 1995, IBVS, No. 4225
Herbig, G. 1985, ApJ, 289, 269
Hill, G., Fisher, W., & Holmgren, D. 1989, A&A, 218, 152
Hoffmann, M. 1982, A&AS, 47, 561
Kitamura, M., Nakamura, T., & Takahashi, C. 1957
Kjurkchieva, D., Marchev, D., & Zola, S. 2002, A&A, 386, 548
Kjurkchieva, D., Marchev, D., & Ogloza, W. 2003a, A&A, 400, 623
Kjurkchieva, D., Marchev, D., & Zola, S. 2003b, A&A, 404, 611
Kjurkchieva, D., Marchev, D., & Ogloza, W. 2004, A&A, 415, 231
Koch, R. 1967, AJ, 213, 458
Kreiner, J., Kim, C., Nha Il-Seong 2001, An Atlas of O–C Diagrams of Eclipsing Binary Stars (Krakow Pedagogical University Press)
Landolt, A. 1983, AJ, 88, 439
Lazaro, C., & Arevalo, M. 1997, AJ, 113, 2283
Montes, D., Fernandez-Figueroa, M., De Castro, E., & Cordine, M. 1994, A&A, 285, 609
Montes, D., Fernandez-Figueroa, M., De Castro, E., & Cordine, M. 1995, A&A, 294, 165
Popper, D. 1995, IBVS, No. 4185
Popper, D. 1997, AJ, 114, 1195
Scaltriti, F., Cellino, A., & Busso, M. 1985, A&A, 149, 11
Smirnov, O., Piskunov, N., Afanasyev, V., & Morozov, A. 1992, In Astronomical Data Analysis Software and Systems 1, ASP Conf. Ser., 26, 344
Strassmeier, K., Fekel, F., Bopp, B., Dempsey, R., & Henri, G. 1990, ApJS, 72, 191
Strassmeier, K., Hall, D. S., Kekel, F. C., & Schenk, M. 1993, A&AS, 100, 173
Vincent, A., Piskunov, N., & Tuominen, I. 1993, A&A, 278, 523
Zarro, D., & Rogers, A. 1983, ApJS, 53, 815
Zeilik, M., Cox, D. A., De Blasi, C., Rhodes, M., & Budding, E. 1989, ApJ, 345, 991
Zeilik, M., Ledlow, M., Rhodes, M., Arevalo, M., & Budding, E. 1990, ApJ, 354, 352
Zhai, D., Qiao, G., & Zhang, X. 1990, A&A, 237, 148
Xiang, F., & Liu, Q. 1997, A&AS, 124, 281
Xiang, F., Deng, S., & Liu, Q. 2000, A&AS, 146, 7

Online Material

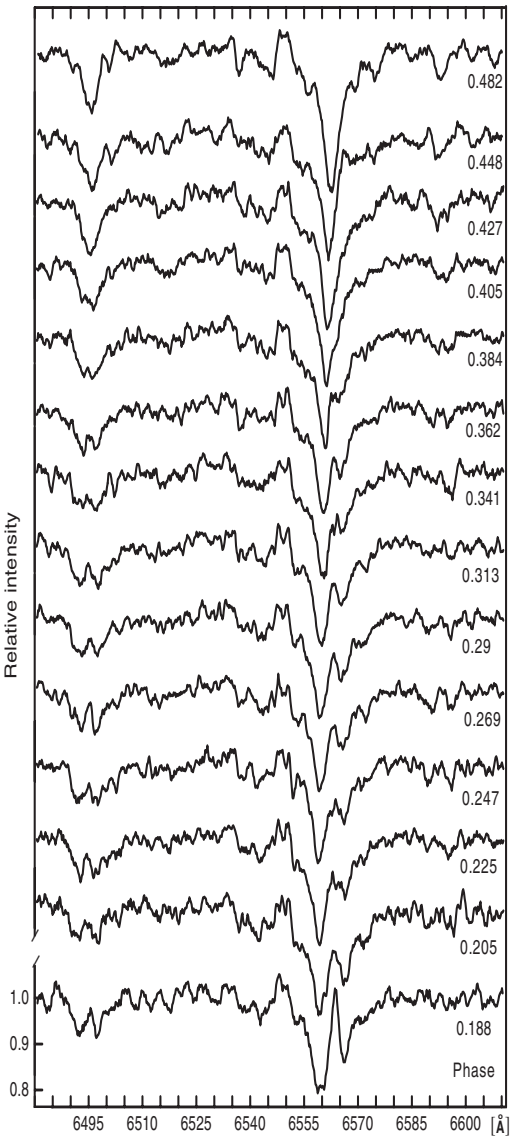

Fig. 2. The spectra of BH Vir from April 8.

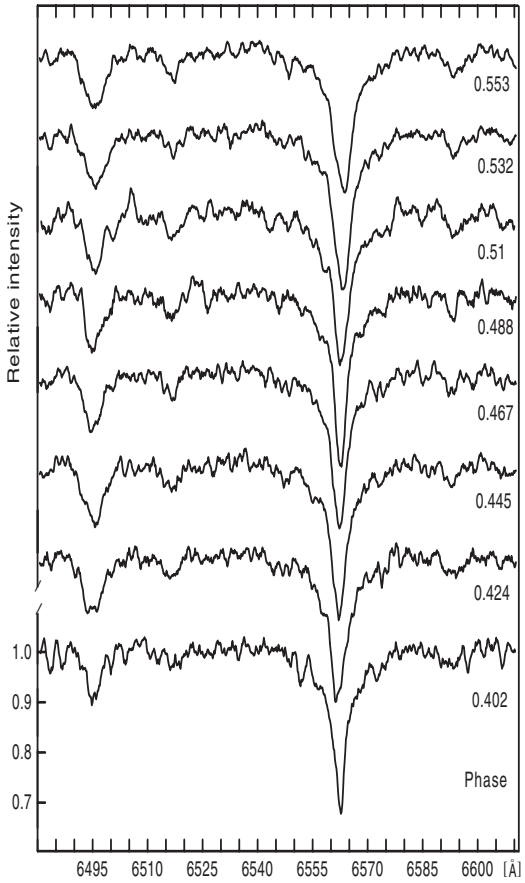

Fig. 3. The spectra of BH Vir from April 9.

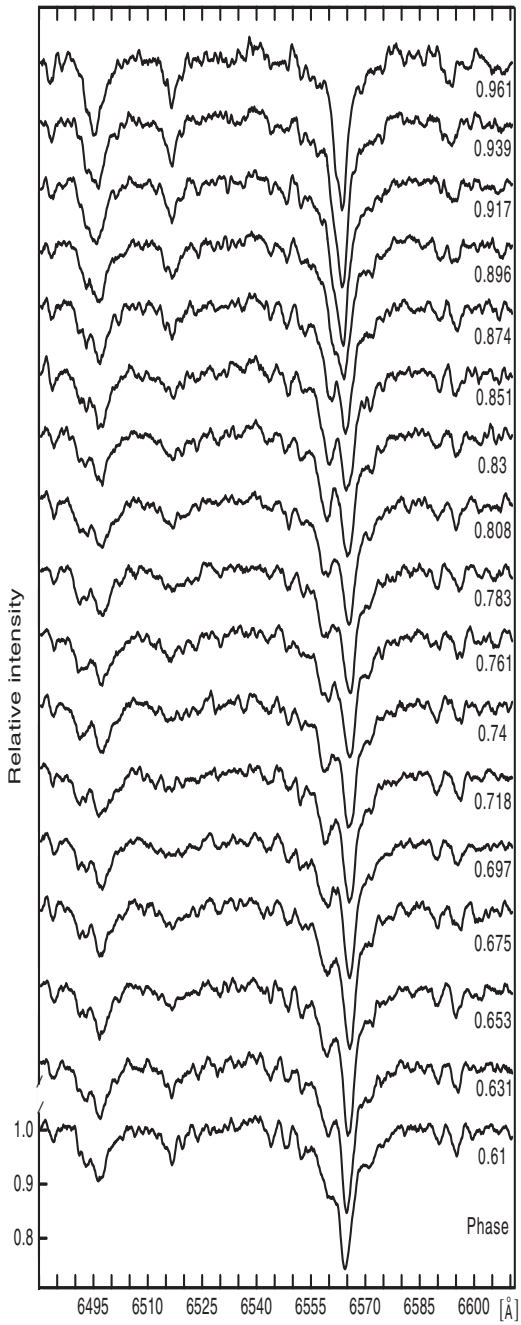

Fig. 4. The spectra of BH Vir from May 7.

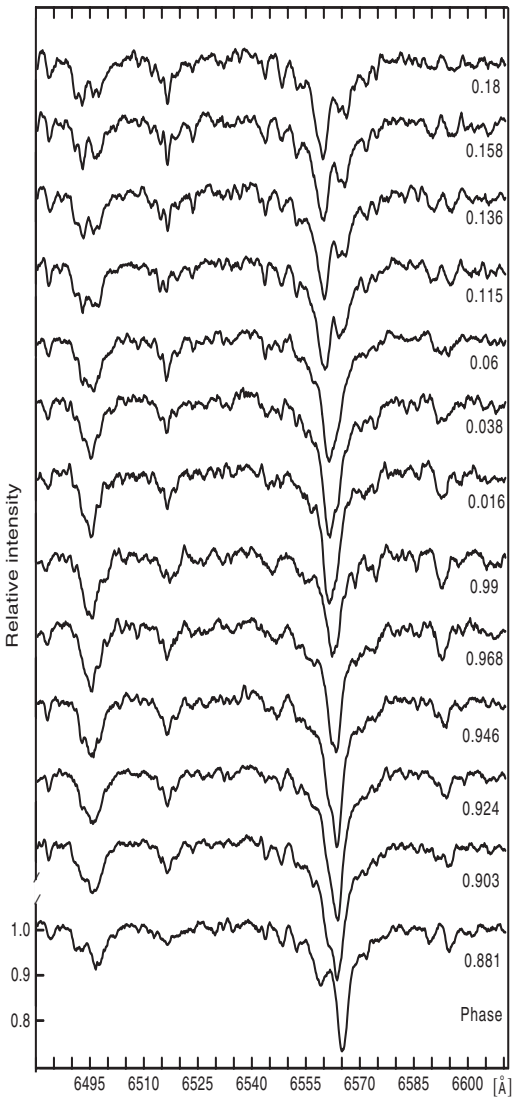

Fig. 5. The spectra of BH Vir from May 8.

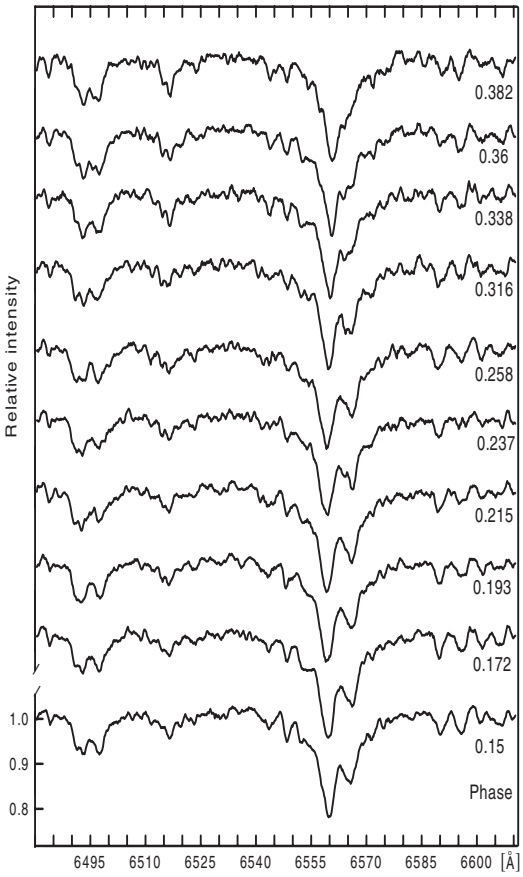

Fig. 6. The spectra of BH Vir from May 9.

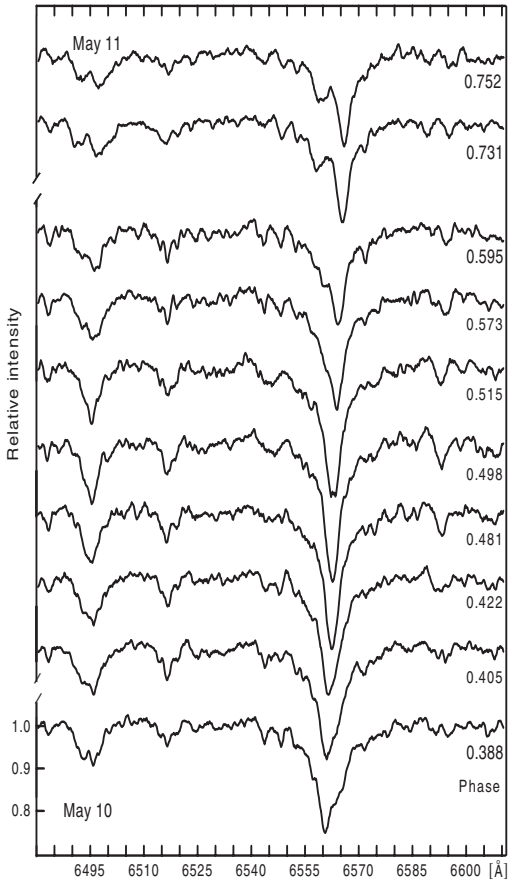

Fig. 7. The spectra of BH Vir from May 10 and 11.

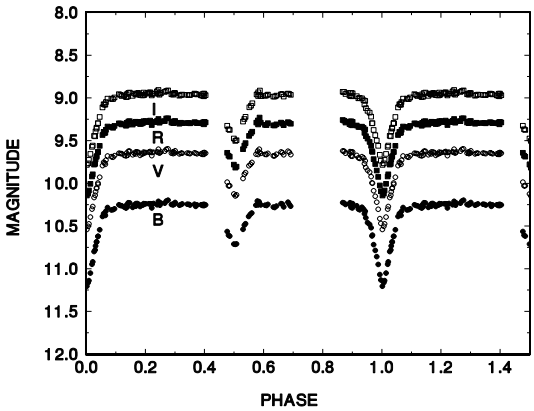

Fig. 9. The light curve of BH Vir in 1996.

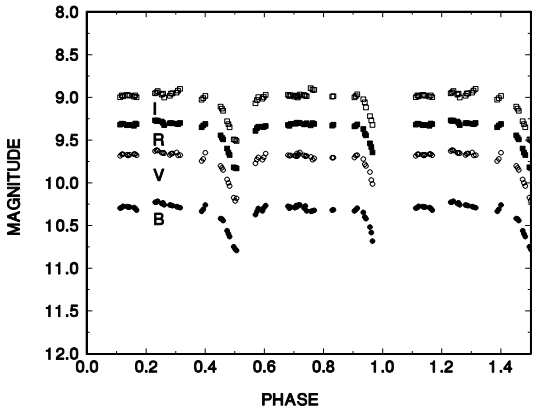

Fig. 10. The light curve of BH Vir in 1997.

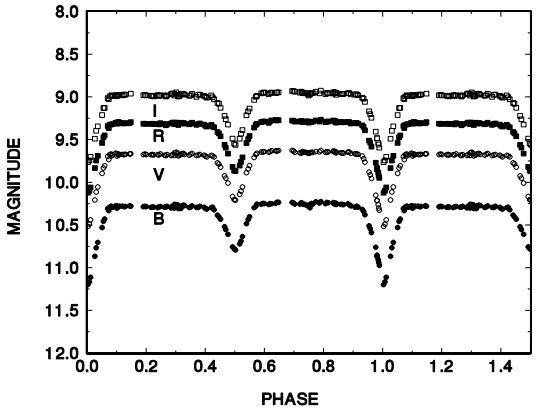

Fig. 11. The light curve of BH Vir in 1998.

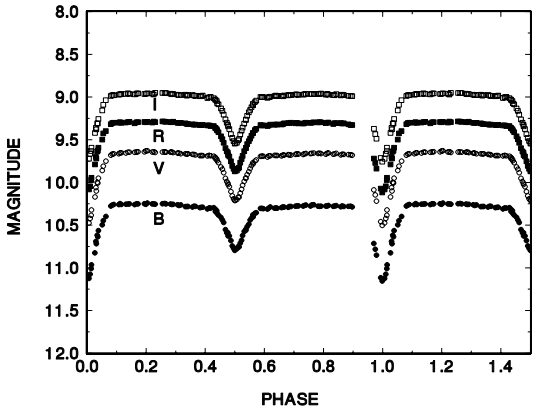

Fig. 12. The light curve of BH Vir in 1999.

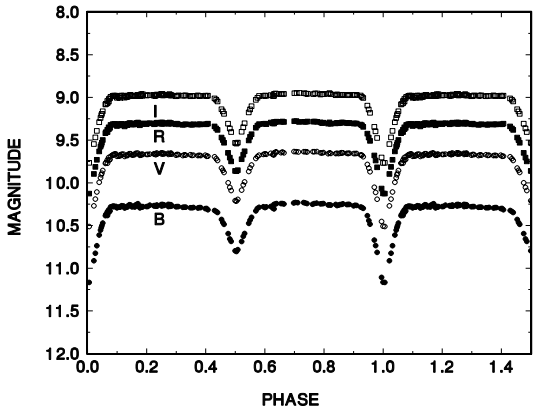

Fig. 13. The light curve of BH Vir in 2000.

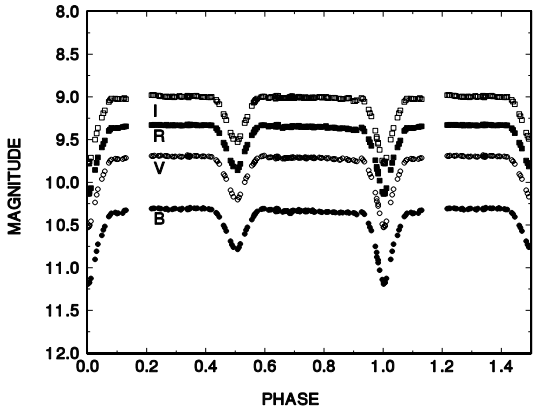

Fig. 14. The light curve of BH Vir in 2001.

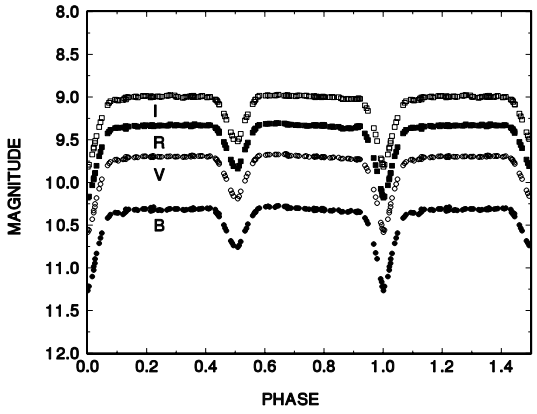

Fig. 15. The light curve of BH Vir in 2002.

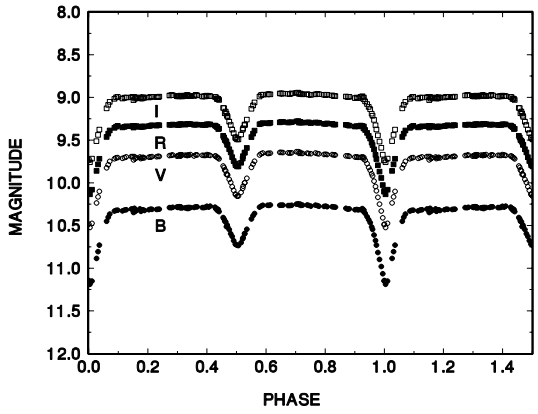

Fig. 16. The light curve of BH Vir in 2003.